Journal of Modern Optics
Vol. 53, Nos. 1–2, 10–20 January 2006, 75–85

Taylor & Francis
Taylor & Francis Group

Self-compression of ultra-short laser pulses down to one optical cycle by filamentation

A. COUAIRON*†, J. BIEGERT‡, C. P. HAURI‡, W. KORNELIS‡, F. W. HELBING‡, U. KELLER‡ and A. MYSYROWICZ§

†Centre de Physique Théorique, École Polytechnique, CNRS UMR 7644, F 91128 Palaiseau Cedex, France
‡ETH Zürich, Physics Department, IQE, 8093 Zürich, Switzerland
§Laboratoire d'Optique Appliquée, École Nationale Supérieure des Techniques Avancées–École Polytechnique, F-91761 Palaiseau Cedex, France

(*Received 27 February 2005; in final form 2 June 2005*)

Theoretical studies of filamentation of ultra-short near-IR laser pulses propagating in a noble gas predict near single-cycle pulses with the intensity being clamped to the field ionization threshold. Experimental results show that this method is carrier envelope offset phase preserving and provides a very simple source for generating few-cycle intense laser pulses. This suggests a very simple design for the generation of ultra-short, sub-femtosecond XUV optical pulses.

1. Introduction

The pursuit of ever shorter optical pulses continues unabated [1–4]. By up-converting the optical frequencies into the extreme ultraviolet (XUV) region, single sub-femtosecond pulses have been generated [5–7]. This approach requires driving the atoms into a strong nonlinear regime with intense few-cycle infra-red (IR) laser pulses. The atoms in turn re-radiate part of the incoming light in the form of high-order odd harmonics [8, 9]. An instructive semi-classical model [10, 11] nicely captures the basic physics of the process. For a sufficiently strong amplitude of the laser field, a peripheral electron is liberated from the atom. The motion of the electron wave packet originating in the continuum is then driven by the remaining laser electric field. For an appropriate time of birth with respect to the optical phase of the pulse, part of the electron wave packet returns to the parent ion with maximum kinetic energy, which can be released in the form of a brief XUV photon burst. Based on this scheme, an ensemble of atoms have been shown to emit single XUV pulses as short as 250 attoseconds (1 as $\equiv 10^{-18}$ s) [7].

*Corresponding author. Email: couairon@cpht.polytechnique.fr

Journal of Modern Optics
ISSN 0950–0340 print/ISSN 1362–3044 online
http://www.tandf.co.uk/journals
DOI: 10.1080/09500340500227760

To obtain isolated attosecond pulses, however, the pump laser must satisfy demanding conditions: the pulse duration must be sufficiently short such that the field strength to liberate an electron is reached during one or two optical cycles only. On the other hand, the laser intensity must be adjusted such that the threshold of field ionization occurs near the crest of an optical cycle. An additional requirement therefore is that the carrier-envelope offset (CEO) phase is locked [12, 13].

Currently, the only proven way to produce CEO phase-locked few-cycle pulses proceeds via self-phase modulation of already CEO phase-locked 30–50 fs pulses, propagating in a long guiding structure (hollow fibre) filled with a neutral gas [14, 15]. Self-phase modulation adds new red frequency components to the leading and blue components on the trailing edge of the pulse. Typically, chirped mirrors are used to suitably retard the red with respect to the blue components, which will lead to the desired few-cycle pulse [16, 17]. The drawback of this method stems from the hollow fibre, which is very sensitive to alignment [18] and is limited in its energy throughput. The emerging pulse is focused into a gas target, usually a noble gas.

The aim of this paper is to show that, under suitable conditions, propagation in a noble gas of a femtosecond pulse, from commercially available lasers with energy in the mJ range, generates pulses nearly as short as one optical cycle with a few hundreds of μJ energy by itself. This phenomenon relies on the now well known process of filamentation [19–24]. We show for the first time that filamentation can be tuned to reach very efficient pulse self-compression down to one optical cycle, a result that might highly impact several domains related to high-field physics. The advantage of this scheme is its simplicity: no specific optical system is needed in order to guide and self-compress the pulse and the intensity is sufficient to ionize atoms. In fact, due to the complex interplay between self-focusing of the beam by the optical Kerr effect and defocusing by multi-photon ionization [19], the intensity is automatically clamped to the proper value for obtaining harmonics of orders up to 23 in argon [25].

2. Modelling self-compression by filamentation

The typical configuration we consider is the propagation of a Gaussian laser pulse with a central wavelength of $\lambda_0 = 800\,\text{nm}$, energy of $E_{\text{in}} = 1.1\,\text{mJ}$, beam radius ($1/e^2$ half width) $w_0 = 2.25\,\text{mm}$ and duration $\tau_{\text{FWHM}} = 25\,\text{fs}$, focused in a gas cell filled with argon at a pressure of $p = 780\,\text{mbar}$. For the sake of completeness, we take propagation of the pulse over 27 cm in air at atmospheric pressure into account, before entering the 160 cm long gas cell; the focus is centred in the middle of the cell ($f = 107\,\text{cm}$). The input pulses are assumed to be cylindrically symmetric.

Our code solves the nonlinear envelope equation describing the forward propagation along the z axis of the laser pulse [24]

$$U\frac{\partial\tilde{\mathcal{E}}}{\partial z} = \frac{i}{2k}\left[\nabla_\perp^2 + \frac{n^2\omega^2}{c^2} - k^2U^2\right]\tilde{\mathcal{E}} + \text{FT}\{N(\mathcal{E})\}, \tag{1}$$

where $k = n_0\omega_0/c$ and ω_0 are the wavenumber and frequency of the carrier wave, n_0 denotes the refractive index at ω_0, $U(\omega) \equiv 1 + (\omega - \omega_0)/kv_g$, $v_g \equiv \partial\omega/\partial k|_{\omega_0}$ denotes the group velocity, $\tilde{\mathcal{E}}(r, \omega, z) \equiv \mathrm{FT}(\mathcal{E}(r, t, z))$ and FT is the Fourier transform. This is equivalent to the model derived by Brabec and Krausz [26], where equation (1) is expressed in the frequency domain, corresponding to the retarded time $t \equiv t_{\mathrm{lab}} - z/v_g$. Numerical solutions of equation (1) have been shown to accurately reproduce the propagation of laser pulses with duration down to one optical cycle (2.6 fs) [26]. This model and the present simulations are fully three dimensional, combining the advantages of a tractable extended model valid for few-cycle pulses with a correct description of all effects responsible for pulse shortening. In this respect, diffraction in the transverse plane and self-focusing have been shown to play a crucial role in pulse restructuring. However, the model also accounts for group velocity dispersion, and high-order dispersive effects, self-focusing with a delayed component in the Kerr effect (to account for stimulated molecular Raman scattering in air), absorption and defocusing due to the plasma generated by photo-ionization, space–time focusing and self-steepening. The nonlinear terms in the time domain are given as

$$N(\mathcal{E}) = ik_0 n_2 T^2 |\mathcal{E}|^2 \mathcal{E} - \frac{\sigma}{2}(1 + i\omega_0\tau_c)\rho\mathcal{E} - \frac{T}{2}\frac{W_{\mathrm{PI}} U_i(\rho_{\mathrm{at}} - \rho)}{|\mathcal{E}|^2}\mathcal{E}, \tag{2}$$

where $\mathcal{E} = \mathcal{E}(r, z, t)$. The operator $T \equiv 1 + (i/\omega_0)(\partial/\partial t)$ in front of the Kerr term is responsible for self-steepening of the pulse [27]. Below we give the parameters used for the argon cells. Self-focusing occurs for pulses with a power P_{in} above the critical value $P_{\mathrm{cr}} \equiv \lambda_0^2/2\pi n_0 n_2$ $(2.7\,\mathrm{GW}/p)$ with the nonlinear refraction index $n_2^{\mathrm{argon}} = 4.9 \times 10^{-19}\, p\,\mathrm{cm}^2/\mathrm{W}$ [28], where p is expressed in bar. The cross section for inverse Bremsstrahlung follows the Drude model [29] and is calculated according to $\sigma = (ke^2/n_0^2\omega_0^2\epsilon_0 m) \times [\omega_0\tau_c/(1 + \omega_0^2\tau_c^2)]$, with the collision time $\tau_c = 190/p\,\mathrm{fs}$ in argon. The last term in equation (2) describes multi-photon absorption, computed in the framework of Keldysh's model with an intensity-dependent ionization rate $W_{\mathrm{PI}}(|\mathcal{E}|^2)$ [30], neutral argon density $\rho_{\mathrm{at}} = 1.9 \times 10^{19}\,\mathrm{cm}^{-3}$, and potential $U_i = 15.76\,\mathrm{eV}$. For air before the gas cells, we used the parameters as in [24], i.e. $n_2^{\mathrm{air}} = 3.2 \times 10^{-19}\,\mathrm{cm}^2/\mathrm{W}$, $\tau_c = 350\,\mathrm{fs}$ and $U_i = 12.06\,\mathrm{eV}$ and a Raman contribution was added to the Kerr effect with fraction $f_R = 0.5$, and characteristic time $\tau_R = 70\,\mathrm{fs}$ [31]:

$$N_{\mathrm{Raman}}(\mathcal{E}) = ik_0 n_2 T^2 \left[(1 - f_R)|\mathcal{E}(t)|^2 + f_R \int_{-\infty}^{t} \frac{\mathrm{d}\tau}{\tau_R}\, \mathrm{e}^{(\tau - t)/\tau_R} |\mathcal{E}(\tau)|^2\right]\mathcal{E}(t). \tag{3}$$

Equation (1) is coupled with the evolution equation for the density of the plasma generated by optical field ionization (first term on the right-hand side of equation (4)) and avalanche ionization (second term):

$$\frac{\partial\rho}{\partial t} = W_{\mathrm{PI}}(|\mathcal{E}|^2)(\rho_{\mathrm{at}} - \rho) + \frac{\sigma}{U_i}\rho|\mathcal{E}|^2. \tag{4}$$

3. Predictions of the numerical simulations

Figure 1 shows numerical results for the peak pulse intensity and the electron density as a function of propagation distance. The pulse intensity (continuous curve) is sufficient to ionize the gas, producing a plasma with a constant density of $\sim 10^{17}\,\mathrm{cm}^{-3}$ (dashed curve) over nearly 50 cm. Although temporal splitting and spectral broadening of the pulse significantly modify the dynamics during propagation [22, 32, 33], the peak intensity in the light channel remains clamped to $6 \times 10^{13}\,\mathrm{W/cm}^2$ [34]. We discuss here the generation of substructures in the temporal profiles of the pulse in the so-called low-pressure regime ($p < 1$ bar) where plasma defocusing prevails over other physical effects in counteracting the optical Kerr effect [35]. Plasma defocusing not only splits the pulse, but allows the formation of very short structures of about one optical cycle during the filamentation stage.

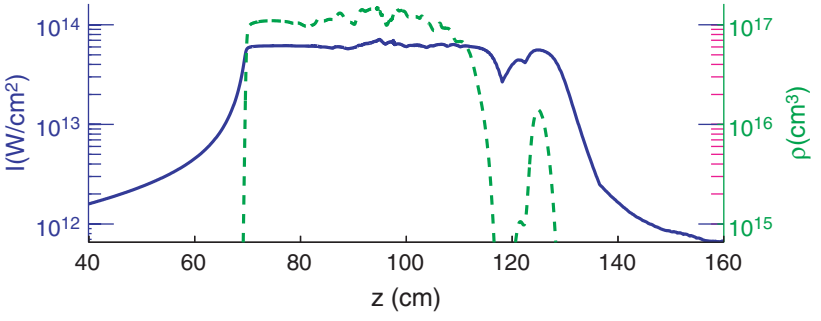

Figure 1. Peak intensity (continuous curve, scale on the left axis) and electron density (dashed curve, scale on the right axis) as a function of propagation distance. The linear focus of the lens is located at $z = 107$ cm. (The colour version of this figure is included in the online version of the journal.)

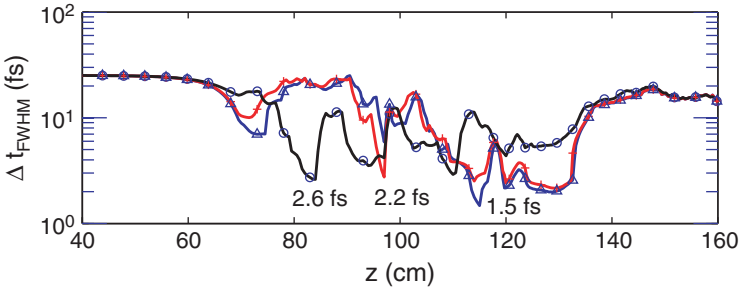

Figure 2. FWHM pulse duration as a function of propagation distance. The initial 1 mJ laser pulse with 25 fs duration is focused in a 160 cm long argon cell at 800 mbar. Three minimal durations reached at 85, 97 and 115 cm are indicated below the minima. The markers indicate that the intensity is averaged over a diameter of 40 μm (triangles), 80 μm (crosses) and 200 μm (circles). Another flat minimum is obtained between 120 and 130 cm and corresponds to the single cycle pulse with duration between 2 and 3 fs. (The colour version of this figure is included in the online version of the journal.)

Figure 2 shows the calculated pulse duration as a function of the propagation distance. The curves marked with circle and crosses indicate the full-width-at-half-maximum (FWHM) duration of the intensity averaged over a diameter of 160 and 80 μm, respectively. We observe that extremely short structures with durations less than 5 fs grow from a background pulse of duration roughly equal to the initial duration. Remarkably, this behaviour is not only obtained for the on-axis intensity, but also for the intensity averaged over a finite diameter.

Figure 3(*a*)–(*d*) show the space–time profiles ($I(r, t)$) of the pulse at different locations inside the filament, corresponding to minima in figure 2. The initially Gaussian pulse quickly transforms into a complex multi-peaked structure which later evolves into a single isolated pulse. Figure 3(*a*) and (*b*) show that the profiles exhibit several substructures in the leading and the trailing part of the pulse. These

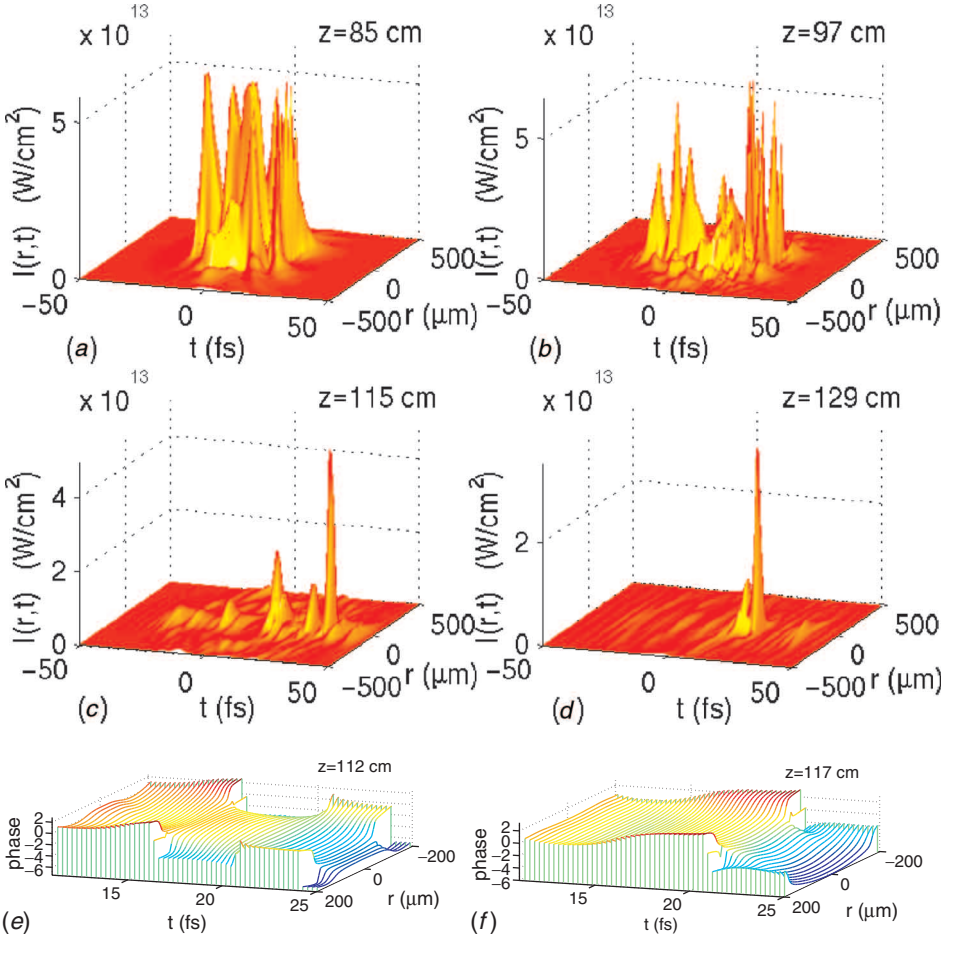

Figure 3. Spatio-temporal intensity distribution at (*a*) 85 cm, (*b*) 97 cm, (*c*) 115 cm and (*d*) 129 cm. (*e*,*f*) Phase front in time and space at $z = 112$ and 117 cm. (The colour version of this figure is included in the online version of the journal.)

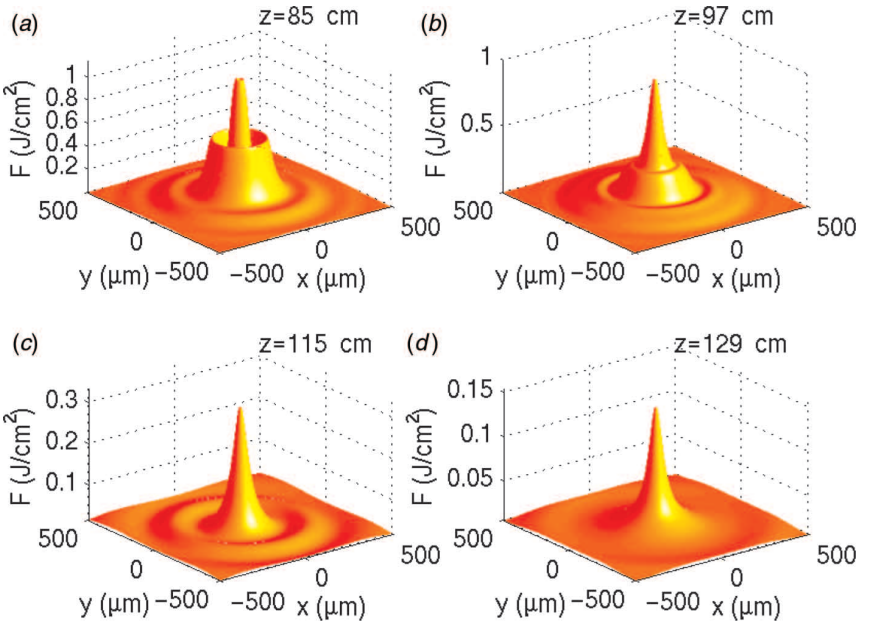

Figure 4. Fluence distribution at (*a*) $z = 85$ cm, (*b*) $z = 97$ cm, (*c*) $z = 115$ cm and (*d*) $z = 129$ cm. (The colour version of this figure is included in the online version of the journal.)

structures are extremely short and the leading peaks are confined to a narrower volume than the trailing peaks. This explains why the temporal profiles, obtained by averaging spatially over 40 μm and 80 μm the intensity distributions shown in figure 3(*a*) and (*b*), remain nearly as short as one optical cycle due to the reduced relative weight of the leading edge. The most striking feature is the fact that an isolated ultra-short structure is formed near the end of the filament. Figure 3(*e*) and (*f*) show the evolution of the associated phase front in time and space. They reveal a nearly flat spatial phase front which also persists over a distance of a few centimetres beyond $z = 115$ cm (see the time slices between 15 and 22 fs in the sequence of figure 3(*e*) and (*f*)), gradually evolving into a quadratic phase front corresponding to a slightly diverging beam.

The respective fluence distributions, defined as the time integrated intensity $F(r, z) \equiv \int_{-\infty}^{+\infty} |\mathcal{E}(r, z, t)|^2 \, dt$, are plotted in figure 4(*a*) and (*b*). We find that the diameter of the central spot oscillates between 80 and 100 μm, and may be surrounded by rings at specific locations (see figure 4(*a*)). Integration of the fluence distribution over a radius of $r_0 = 100$ μm shows that the energy $E_{r=r_0}(z) \equiv \int_0^{r_0} F(r, z) 2\pi r \, dr$ contained in the substructure is of the order of 100 μJ. More precisely, it is equal to 130 and 39 μJ at distances of $z = 85$ and 115 cm, respectively, while the whole beam retains 570 μJ at the end of the filament from $z = 115$ cm. Note here that an important fraction of the input beam energy is not directly available in the single cycle pulse. It nevertheless acts as an energy reservoir from which the intensity in the single cycle pulse is maintained at the ionization threshold, thereby sustaining the conditions for an efficient pulse compression.

We have examined the importance of the initial pulse duration and gas pressure for pulse self-compression and we have found that pulse shortening is rather insensitive to these parameters. Single cycle pulses are obtained with the initial pulse duration varying from 10 to 50 fs. The distance at which the short pulses are generated, however, changes with input pulse duration. Another interesting finding is the insensitivity to gas pressure: for input pulses of 1 mJ, the pressure can be decreased to 100 mbar while still resulting in a similar pulse compression close to one optical cycle. Accordingly, we observe a shift of the position for minimum pulse duration as a function of the gas pressure.

4. Experimental results

In the experiment, filamentation is induced inside two successive 150 cm long cells, filled with argon at pressures of 840 and 700 mbar, by weakly focusing 42 fs, 840 μJ pulses from a CEO-stabilized Ti:Sapphire laser system [36] (see the experimental setup in figure 5). The process preserves the CEO phase of the pump pulse.

In the first gas cell, the pulse generates a 10–20 cm long filament roughly in the centre of the cell, as estimated from the length of the scattered broadband continuum. The emerging spectrum was re-compressed with chirped mirrors, resulting in a shortening by a factor of 4 while retaining 94% (0.79 mJ) of the input energy. Sending the 10.5 fs pulse into the second gas cell, another 15–20 cm long filament was formed, leading, after chirped-mirror re-compression, to a 5.7 fs pulse measured through spectral phase interferometry by direct electric-field reconstruction

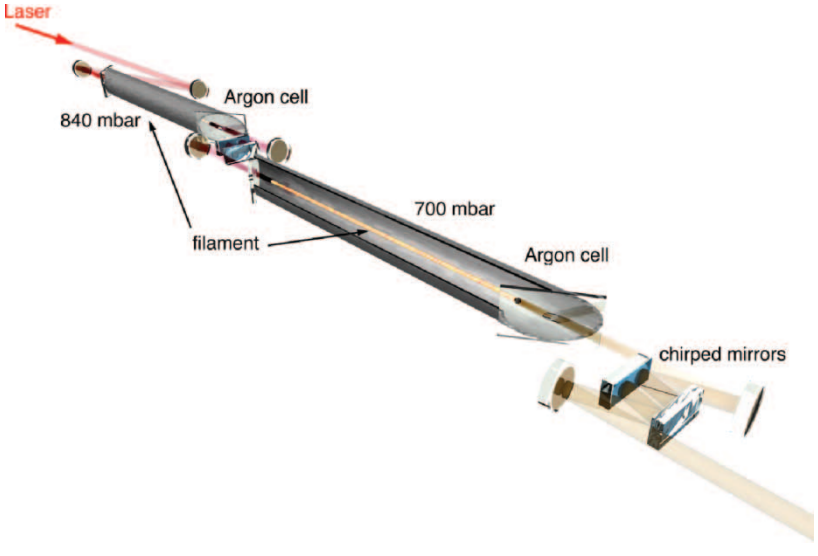

Figure 5. Experimental setup: two cells are filled with argon at 840 and 700 mbar, respectively. CEO phase-locked infra-red pulses with 0.84 mJ energy are sent successively into each gas cell. A re-compression stage in chirped mirrors follows each gas cell. (The colour version of this figure is included in the online version of the journal.)

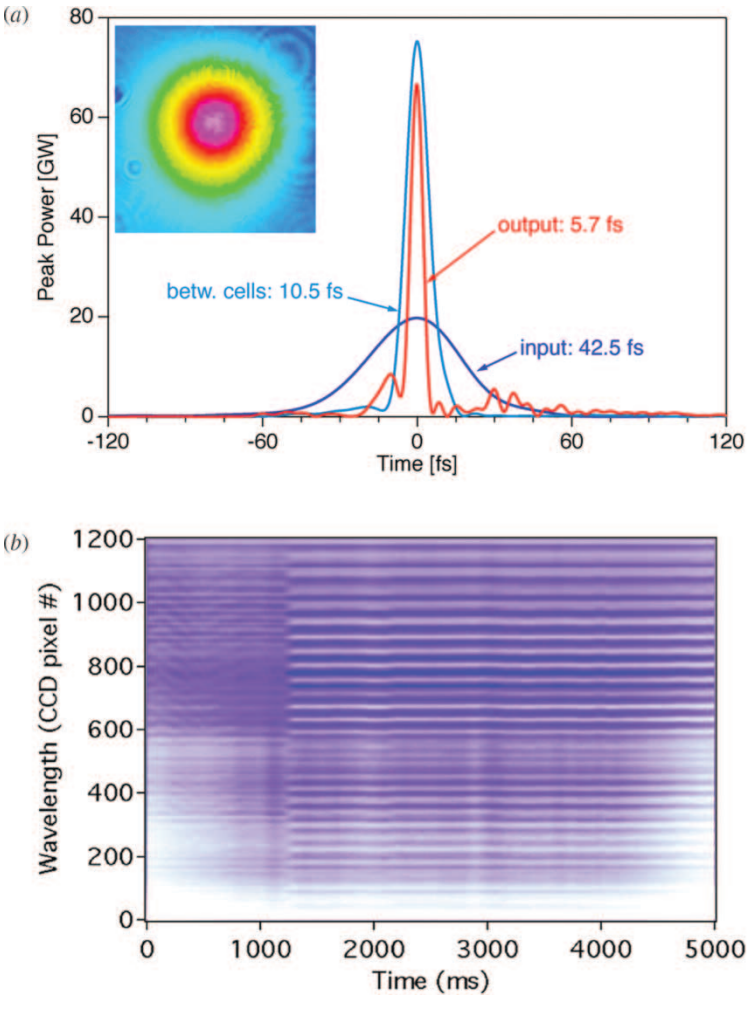

Figure 6. (*a*) Pulse power as a function of time at different distances. The inset shows the excellent beam quality. (*b*) Time series from an *f*–2*f* spectral interferometry measurement. The CEO phase lock is switched on after roughly 1.2 s with the emergence of fringes confirming the CEO phase lock. (The colour version of this figure is included in the online version of the journal.)

(SPIDER [37, 38]). The emerging pulses contain 45% of the initial pulse energy in an excellent spatial mode.

Figure 6 shows a comparison of the measured input and output pulse powers as well as the pulse duration between the cells. We note that the minimum value of 5.7 fs is limited by the phase characteristics and bandwidth of the chirped mirrors. For an optimized pressure of 1040 mbar, the pulse spectrum measured before compression theoretically supported a 1.75 fs transform-limited pulse. Roughly 390 μJ of the beam energy was contained in a diverging mode of excellent quality and reproducibility as shown in the inset of figure 6.

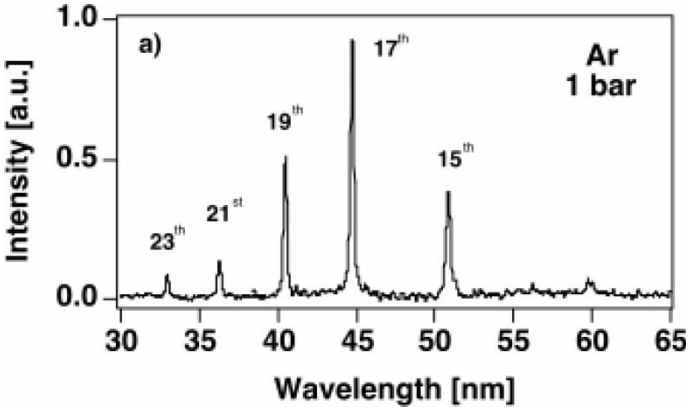

Figure 7. Selective high-harmonic generation by filamentation in argon at 1 bar from 23th to 15th orders.

CEO phase stability is confirmed through *f*–2*f* spectral interferometry [13, 39] with the persistence of fringes confirming the phase-preserving nature of the filaments. Figure 6(*b*) shows the time series of such a measurement where the CEO lock was switched on after roughly 1.2 s. The measurement clearly confirms the formation and steadiness of the fringes, hence corroborating CEO phase conservation.

Pulse self-shortening by filamentation suggests its application to attosecond pulse generation via high-order harmonic generation with the considerable advantage being the simplicity of the experimental setup: the proper pump pulse characteristics (few-cycle duration, intensity control to the field ionization onset) are implicitly realized without any critical adjustment, simply by gently focusing relatively long (42 fs) IR pulses from a commercially available Ti:Sapphire laser system into a gas cell filled with argon. Furthermore, the harmonic efficiency should benefit from the long interaction path of a pulse with a nearly flat phase front [25]. Tamaki *et al*. [25] have shown an important enhancement of high harmonics in low-pressure gases by using 30 fs pulses with a flat front phase. Another advantage is that the same cell can be used for filamentation as well as for high-order harmonic generation. Results obtained recently in Zürich corroborate this conjecture. Infra-red laser pulses with an energy of 0.8 mJ and a duration of 40 fs were focused into a specially designed 14 cm laser–gas interaction cell inside a vacuum chamber. A filament is generated in the interaction target. During filamentation, high harmonics are generated and detected by a XUV spectrometer after propagating through a differentially pumped vacuum stage. In argon gas at a pressure of 1 bar, we have detected odd harmonics up to 23rd order of the driving laser field. As can be seen in figure 7, the signal amplitude for the 17th harmonic exceeds that of the neighbouring amplitudes by a factor of 2 (19th) or more (other harmonics). Relying on the semi-classical model of Corkum [10], the highest harmonics infer a peak intensity of about 10^{14} W/cm^2 inside the filament, in agreement with our calculation.

In conclusion, a realistic three-dimensional code predicts that intense femtosecond laser pulses propagating in an argon gas cell undergo pulse compression

down to the single cycle limit because of filamentation. Such ultra-short laser pulses should provide ideal pump pulses for the production of attosecond XUV pulses by high-order harmonic generation. Results for pulse self-compression down to 10 fs have recently been published and are in good agreement with our analysis, although the compression technique still uses a fibre to help guiding [40]. Our approach shows that the pulses can be self-compressed further by a factor of at least 2 to 3. The simplicity of our experimental setup as well as the potential to scale up this technique are crucial points which will make CEO-phase-locked single cycle pulses much more accessible to the field of attoscience.

Acknowledgements

J. Biegert, C.P. Hauri and U. Keller acknowledge support from the Swiss National Science Foundation (QP-NCCR), ETH Zürich, and from the EU FP6 program 'Structuring the European Research Area', Marie Curie Research Training Network XTRA (contract No. FP6-505138).

References

[1] T. Brabec and F. Krausz, Rev. mod. Phys. **72** 545 (2000).
[2] U. Keller, Nature **424** 831 (2003).
[3] B. Schenkel, J. Biegert, U. Keller, *et al.*, Optics Lett. **28** 1987 (2003).
[4] G. Steinmeyer, D.H. Sutter, L. Gallmann, *et al.*, Science **286** 1507 (1999).
[5] P.M. Paul, E.S. Toma, P. Breger, *et al.*, Science **292** 1689 (2001).
[6] M. Drescher, M. Hentschel, R. Kienberger, *et al.*, Science **291** 1923 (2001).
[7] R. Kienberger, E. Goulielmakis, B. Uiberacker, *et al.*, Nature **427** 817 (2004).
[8] P. Antoine, A. L'Huillier and M. Lewenstein, Phys. Rev. Lett. **77** 1234 (1996).
[9] A. L'Huillier, K.J. Schafer and K.C. Kulander, J. Phys. B **24** 3315 (1991).
[10] P.B. Corkum, Phys. Rev. Lett. **71** 1994 (1993).
[11] M. Lewenstein, P. Salières and A. L'Huillier, Phys. Rev. A **52** 4747 (1995).
[12] E. Goulielmakis, M. Uiberacker, R. Kienberger, *et al.*, Science **305** 1267 (2004).
[13] H.R. Telle, G. Steinmeyer, A.E. Dunlop, *et al.*, Appl. Phys. B **69** 327 (1999).
[14] M. Nisoli, S. de Silvestri, O. Svelto, *et al.*, Appl. Phys. B **65** 186 (1997); ibid. Optics Lett. **22** 522 (1997).
[15] A. Baltuska, T. Udem, M. Uiberacker, *et al.*, Nature (London) **421** 611 (2003).
[16] P. Laporta and V. Magni, Appl. Optics **24** 2014 (1985).
[17] R. Szipöcs, K. Ferencz, C. Spielmann, *et al.*, Optics Lett. **19** 201 (1994).
[18] W. Kornelis, M. Bruck, F.W. Helbing, *et al.*, Appl. Phys. B **79** 1033 (2004).
[19] A. Braun, G. Korn, X. Liu, *et al.*, Optics Lett. **20** 73 (1995).
[20] E.T.J. Nibbering, P.F. Curley, G. Grillon, *et al.*, Optics Lett. **21** 62 (1996).
[21] A. Brodeur, C.Y. Chien, F.A. Ilkov, *et al.*, Optics Lett. **22** 304 (1997).
[22] M. Mlejnek, E.M. Wright and J.V. Moloney, Optics Lett. **23** 382 (1998).
[23] M. Mlejnek, M. Kolesik, E.M. Wright, *et al.*, Phys. Rev. Lett. **83** 2938 (1999).
[24] G. Méchain, A. Couairon, M. Franco, *et al.*, Phys. Rev. Lett. **93** 035003 (2004).
[25] Y. Tamaki, J. Itatani, Y. Nagata, *et al.*, Phys. Rev. Lett. **82** 1422 (1999); Y. Tamaki, J. Itatani, M. Obara, *et al.*, Phys. Rev. A **62** 063802 (2000); V. Tosa, E. Takahashi, Y. Nabekawa, *et al.*, Phys. Rev. A **67** 063817 (2003).
[26] T. Brabec and F. Krausz, Phys. Rev. Lett. **78** 3282 (1997).
[27] A.L. Gaeta, Phys. Rev. Lett. **84** 3582 (2000).

[28] Y. Shimoji, A.T. Fay, R.S.F. Chang, *et al.*, J. Opt. Soc. Am. B **6** 1994 (1989).
[29] E. Yablonovitch and N. Bloembergen, Phys. Rev. Lett. **29** 907 (1972).
[30] L.V. Keldysh, ZhETF **47** 1945 (1964); Soviet Phys. JETP **20** 1307 (1965).
[31] J.F. Ripoche, G. Grillon, B.S. Prade, *et al.*, Optics Commun. **135** 310 (1997).
[32] A. Couairon, S. Tzortzakis, L. Bergé, *et al.*, J. Opt. Soc. Am. B **19** 1117 (2002).
[33] M. Nurhuda, A. Suda, M. Hatayama, *et al.*, Phys. Rev. A **66** 023811 (2002).
[34] A. Becker, N. Aközbek, K. Vijayalakshmi, *et al.*, Appl. Phys. B **73** 287 (2001).
[35] M. Mlejnek, E.M. Wright and J.V. Moloney, Phys. Rev. E **58** 4903 (1998).
[36] C.P. Hauri, W. Kornelis, F.W. Helbing, *et al.*, Appl. Phys. B **79** 673 (2004).
[37] C. Iaconis and I.A. Walmsley, Optics Lett. **23** 792 (1998).
[38] W. Kornelis, J. Biegert, J.W.G. Tisch, *et al.*, Optics Lett. **28** 281 (2003).
[39] M. Mehendale, S.A. Mitchell, J.P. Likforman, *et al.*, Optics Lett. **25** 1672 (2000).
[40] N.L. Wagner, E.A. Gibson, T. Popmintchev, *et al.*, Phys. Rev. Lett. **93** 173902 (2004).